ELSEVIER

Chemical Engineering Journal 66 (1997) 97–104

Chemical Engineering Journal

Mixing studies in external-loop airlift reactors

Maria Gavrilescu [a], Radu Z. Tudose [b]

[a] *Chemical Pharmaceutical Research Institute, Research Centre for Antibiotics, 6647 - Valea Lupului no. 1, Jassy, Romania*

[b] *Department of Transfer Phenomena and Chemical Engineering, Technical University of Jassy, Mangeron Str. no. 71, 6600 Jassy, Romania*

Received 7 August 1995; accepted 17 October 1996

Abstract

The mixing behaviour of the liquid phase in two external-loop airlift reactors of laboratory and pilot scale, in terms of the mixing time and axial dispersion, was investigated. The mixing parameters were determined from the output curves to an initial Dirac pulse, using the classical tracer response technique, and analysed in relation to operating and geometrical parameters, such as v_{sGR}, A_D/A_R, H_d and D_R. Mixing in the external-loop airlift reactors under investigation was essentially correlated with the liquid circulation velocity. The specific sections of the airlift reactor have different mixing behaviour, so that the riser and downcomer can be analysed as plug flow with axial dispersion, whereas the top section approaches ideal mixing behaviour. A simple correlation between the specific mixing time and the operating and geometrical parameters was developed which can be used for design and scale-up purposes. © 1997 Elsevier Science S.A.

Keywords: External-loop airlift reactor; Liquid phase; Mixing behaviour

1. Introduction

Airlift reactors are currently gaining increasing interest for application in chemical engineering and biotechnology due to their advantages of good mass and heat transfer, high fluid circulation rate, short mixing times and low shear rates.

Mixing is a parameter of particular importance for design, modelling and operation, as well as for scale-up from laboratory to industrial scale, since the time spent in each of the environments that the reactor offers and the age of other elements that an element of fluid contacts are of crucial importance for evaluating the airlift performance [1,2].

Results on mixing time investigations in airlift reactors have been reported in the literature [1–12].

Most of the work dealing with the study of liquid phase dispersion coefficients in airlift reactors has attempted to characterize the liquid phase mixing in terms of an overall axial dispersion coefficient for the whole reactor. Single-parameter models have been used for the description of the overall liquid mixing [1,8,11]. It is essential to understand not only the mixing behaviour of the reactor as a whole, but also that of its different sections (riser, gas-disengagement and downcomer), since the different zones of the airlift reactor are hydrodynamically different [1,2,7].

A large number of investigations of mixing have been performed with laboratory-scale external-loop airlift reactors, but few results have been published on pilot-plant and industrial-scale equipment [1,4,6,7,12]. In addition, the translation of laboratory data to pilot and industrial reactors has been reported only rarely.

This work was undertaken in order to investigate the liquid phase mixing characteristics of two external-loop airlift reactors (one of laboratory scale (EALR-L) and the other of pilot scale (EALR-P)) using the tracer injection technique. The effects of the operating parameters (aeration rate, downcomer-to-riser cross-sectional area, dispersion height, scale of operation) on liquid mixing for the reactor as a whole and for the individual sections were examined extensively. In addition, equations which correlate experimental laboratory and pilot data were developed.

2. Experimental details

Two experimental external-loop airlift reactors (laboratory scale made of glass and pilot scale made of stainless steel), which operated with air and water, were used. Each configuration consisted of two vertical columns connected at the top and the base by horizontal piping containing valves. The geometrical characteristics of the devices are given in Table 1 and illustrated in Fig. 1.

A porous plate sparger was used as gas distributor in EALR-L and a multiring sparger was employed in EALR-P. The contactors were operated successively with different

PII S1385-8947(96)03177-6

Table 1
Characteristics of the external-loop airlift reactors used for mixing studies

Characteristic	Reactor scale				
	Laboratory (EALR-L)			Pilot (EALR-P)	
Material	Glass	Glass	Glass	Stainless steel	Stainless steel
A_D/A_R	1.000	0.360	0.111	0.1225	0.040
D_R (m)	0.030	0.030	0.030	0.200	0.200
D_D (m)	0.030	0.018	0.010	0.070	0.040
H_R (m)	1.160	1.160	1.160	4.70	4.70
H_D (m)	1.100	1.100	1.100	4.40	4.40
$V_L \times 10^3$ (m^3)	1.880	1.382	1.189	170	157
V_R/V_L	0.436	0.593	0.693	0.871	0.943

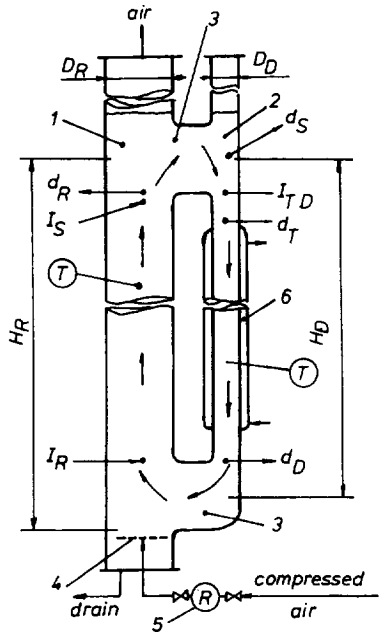

Fig. 1. Experimental set-up: 1, riser; 2, downcomer; 3, connecting pipes; 4, sparger; 5, rotameter; 6, jacket; I, injection point of tracer for mixing studies in the whole airlift reactor (T) and in the separate sections (D, R, S); d, detection point of tracer; T, thermometer.

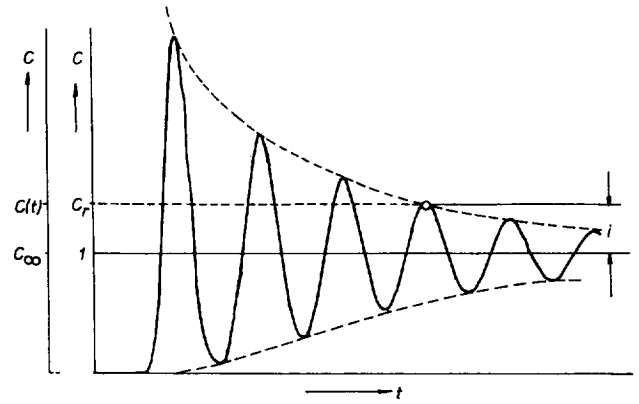

Fig. 2. Determination of the inhomogeneity i characterizing the upper envelope curve connecting the maxima of the impulse distribution.

values of A_D/A_R in the range 0.111–1.000 for EALR-L and at 0.040 and 0.1225 for EALR-P.

The gas superficial velocity in the riser was varied in the range 0.016–0.177 m s^{-1} in the laboratory reactor and 0.01–0.12 m s^{-1} in the pilot contactor. No significant recirculation of gas bubbles into the downcomer was observed. The temperature was maintained at 23 ± 1 °C. The reactors work in batch mode.

The circulation time, mixing time and axial dispersion parameters were determined using the classical tracer response technique [13]. Tracers consisting of 5 ml of methyl orange solution (2.6 mg l^{-1}), analysed by a colorimetric method, in EALR-L, 5 ml of saturated NaCl solution in EALR-L and 20 ml in EALR-P, analysed by a conductometric assay, were injected. The mean deviation of the two methods used in EALR-L was less than 5%.

Discussions are only of value when based on the same degree of mixing, which was determined by the inhomogeneity, defined as shown in Fig. 2 and Eq. (1)

$$i = \frac{C(t) - C_\infty}{C_\infty} = C_r - 1 \tag{1}$$

The mixing time was determined directly from the tracer response curves for a certain degree of inhomogeneity between 5% and 20%. Most of the results were obtained for an inhomogeneity of 5%.

The liquid velocity in a certain region of the reactor was determined as the ratio of its length and the mean residence time for that region of the liquid phase.

The circulation time was determined as the mean time interval between two consecutive peaks of maximum concentration.

The axial dispersion model was used to estimate the axial dispersion number in the airlift reactors

$$\frac{\partial C_r}{\partial \tau} = \frac{1}{\mathrm{Bo}} \frac{\partial^2 C_r}{\partial \tau^2} - \frac{\partial C_r}{\partial x} \tag{2}$$

The solution of Eq. (2) for an initial Dirac pulse in the airlift reactors, considering the circulating flow, is given by [13]

$$C_r = \left(\frac{\mathrm{Bo}}{4\pi\tau}\right)^{1/2} \sum_{x=1}^{\infty} \exp\left[-\frac{(x-\tau)^2 \mathrm{Bo}}{4\tau}\right] \tag{3}$$

Fitting the model to an experimental response for an initial Dirac pulse yields the Bodenstein number for the reactor, calculated for a minimum standard deviation between the predicted and experimental outlet concentration profile, according to the least-square criterion.

For each reactor compartment, the predicted outlet concentration profile was determined by convoluting the experimental inlet concentration profile with the curve calculated for an open–open vessel as a function of Bo [13]. Data were subjected to time domain analysis using the procedure to make periodic the non-periodical functions (such as damped oscillations) proposed by Verlaan [1] and the algorithm for Bo prediction proposed by Lu et al. [10].

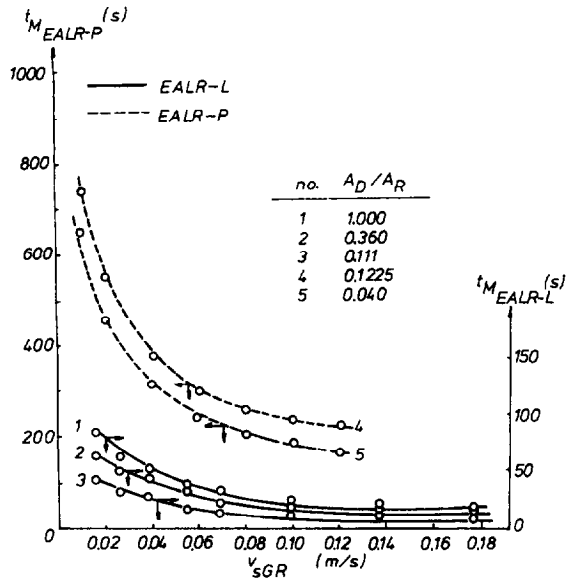

Fig. 3. Dependence of the mixing time on the gas superficial velocity.

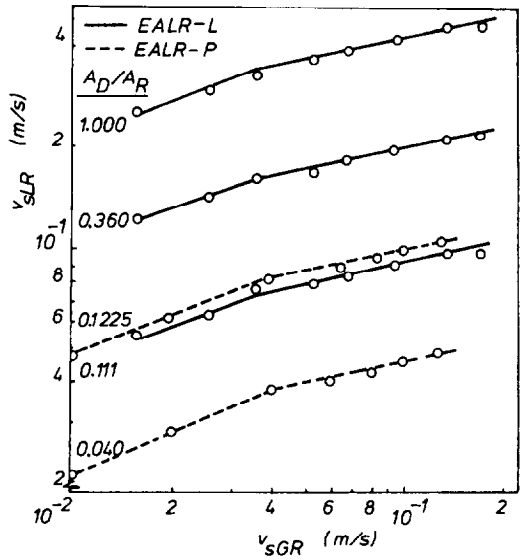

Fig. 4. Liquid circulation time vs. gas superficial velocity.

3. Results and discussion

3.1. Mixing time

The mixing characteristics of airlift reactors of different configurations and scales can be compared by considering the time required to achieve a certain degree of mixing. The mixing time may also be used as an operation and scale-up parameter, its variation being dependent on the operation and geometrical parameters.

The mixing times are strong functions of the gas superficial velocity: up to a v_{sGR} value between 0.04 and 0.06 m s^{-1}, the mixing improves rapidly, whereas at higher gas velocities, the liquid mixing time becomes less efficient, especially in EALR-L (Fig. 3). These values of the gas velocity correspond to the transition from the circulating to the turbulent regime. From Fig. 3, it is evident that the A_D/A_R ratio and the scale of operation exert important influences on t_M. This is a consequence of the effect of v_{sGR} on v_{sLR} and due to the fact that the mixing time is directly correlated with the liquid circulation velocity. A similar behaviour is also observed for the circulation time (Fig. 4). The theory and practical implications of the recirculating liquid velocity in EALRs have been discussed elsewhere [14]. Fig. 5 shows the variation of the liquid superficial velocity with the gas superficial velocity for different A_D/A_R ratios in both EALR-L and EALR-P. The effect of A_D/A_R on t_M in the investigated EALRs can therefore be attributed mainly to the effect of A_D/A_R on the recirculating liquid velocity, which proves to be the physical parameter which most strongly affects the recirculation rates in airlift reactors [15]. Therefore the mixing time can be considered as a measure of the macroscale mixing promoted by convective mechanisms.

To predict or compare the mixing times in an airlift system which is being designed or simulated, as a function of the operating variables and geometry, the specific mixing time, denoted as the mixing time per unit liquid volume (t_M/V_L), is used. The specific mixing time concept has previously been used successfully by Rousseau and Bu'Lock [16] and Popovic and Robinson [6]. Fig. 6 shows the specific mixing time as a function of the liquid superficial velocity in the riser for both EALR-L and EALR-P and all A_D/A_R ratios investigated. In a log–log plot, straight lines are obtained with the slope approximately equal. Since the riser section is an actively sparged zone, an increase in the riser liquid volume will promote more mixing and will cause a shorter specific mixing time.

The scale of operation also exhibits an influence on the specific mixing time (Fig. 6).

On the basis of literature data [5,6,12] and our own investigations [14,17], it was found that the liquid superficial

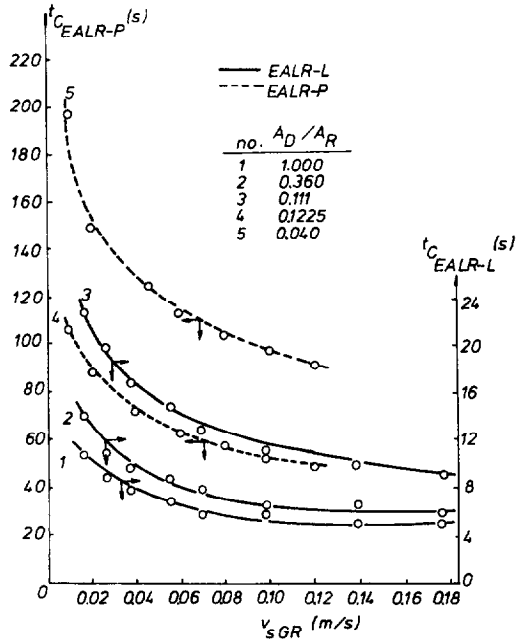

Fig. 5. Liquid circulation velocity vs. gas superficial velocity.

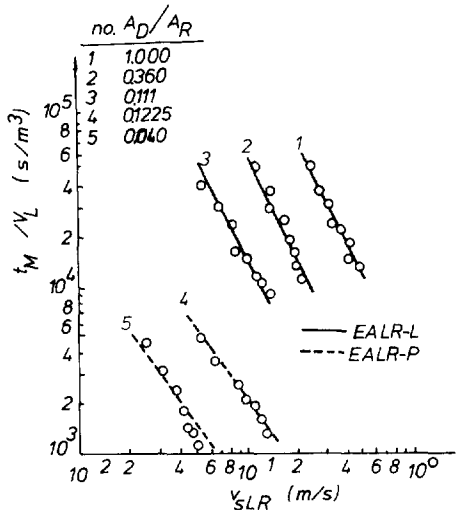

Fig. 6. Specific mixing time (t_M/V_L), measured in EALR-L and EALR-P, for different values of the A_D/A_R ratio as a function of the liquid superficial velocity in the riser v_{sLR}.

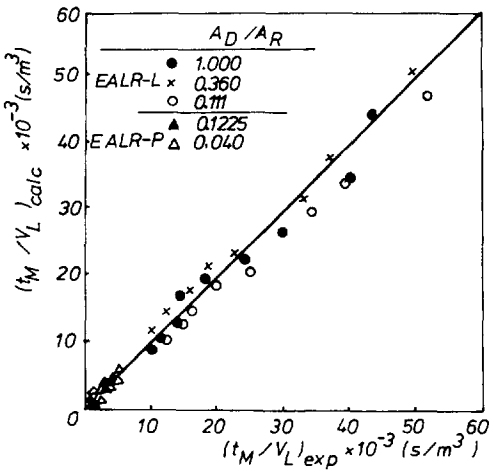

Fig. 7. Comparison of the experimental and calculated (with Eq. (4)) specific mixing times ($i = 0.05$).

velocity in the riser is a function of the dispersion height, the dependence being the same for both bubbly and heterogeneous flow. Therefore the specific mixing time will also be dependent on H_d.

In spite of the fact that v_{sGR} incorporates the influence of the reactor geometry (A_D/A_R, D_R, H_d) and the operating parameter v_{sGR}, it is obvious that the specific mixing time cannot be defined solely by v_{sLR} for all EALR geometries studied. All the experimental data on the mixing time obtained in this work were correlated using the above considerations, by non-linear regression, resulting in the following dependence

$$t_M/V_L = 1100 v_{sGR}^{-0.5} (A_D/A_R)^{0.14} H_d^{-0.78} D_R^{-0.5} \quad (4)$$

with a correlation coefficient of 0.894. Mixing time values were taken for 5% inhomogeneity. The range of experimental data used to develop Eq. (4) was as follows: $v_{sGR} = 0.010$–0.178 m s^{-1}; $v_{sLR} = 0.02$–0.45 m s^{-1}; $A_D/A_R = 0.04$–1.00; $H_R/D_R \geq 20$; $V_L = 1.18 \times 10^{-3}$–$0.17$ m^3.

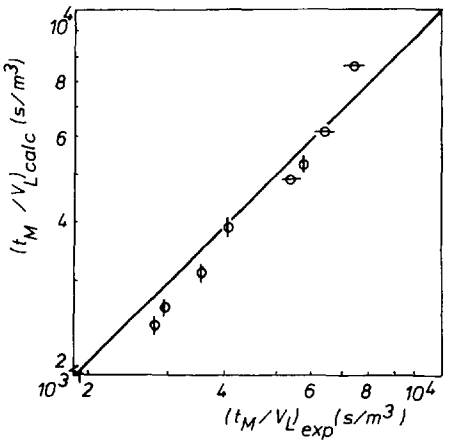

Fig. 8. Comparison of the specific mixing times obtained from the experimental data of Weiland [18] (ϕ: $H_R = 8.5$ m; $D_R = 0.1$ m; $D_D = 0.05$ m; $A_D/A_R = 0.25$; $V_L = 0.0834$ m^3) and Lin et al. [3] (–■–: $H_R = 3.04$ m; $D_R = 0.076$ m; $D_D = 0.026$ m; $H_R/D_R = 40$; $V_L = 0.0154$ m^3) with those calculated using Eq. (4).

A parity plot of Eq. (4) is presented in Fig. 7. The majority of the measured data can be predicted by Eq. (4) with an average error of ±15%. In Fig. 8, the values of the experimental specific mixing time obtained from the results reported by Weiland [18] and Lin et al. [3], compared with those calculated using Eq. (4), are presented. It is evident that Eq. (4) yields good correlation between the experimental data and the operational and geometrical parameters, with an average error of ±15%, being appropriate for scale-up purposes.

3.2. Axial dispersion

Fig. 9 shows a comparison of the outlet response curves, obtained for three different zones and for the reactor as a whole, with the predicted curves. The agreement is very close; therefore an accurate estimation of the Bodenstein number can be made for each section. It is evident that each of the three different sections of the airlift reactor exhibits individual and interrelated mixing behaviour, different from that of the reactor as a whole.

As expected, the gas superficial velocity is the main parameter determining the axial dispersion. Fig. 10 shows the overall Bo number for the whole range of aeration rates used in this study.

The liquid axial dispersion in the external-loop airlift reactors under investigation in this work can be described using the axial dispersion model with Bo numbers in the range 16–110, values which are dependent on the gas superficial velocity, A_D/A_R ratio and the scale of operation. The Bo number decreases with an increase in the gas superficial velocity, this being more noticeable up to $v_{sGR} = 0.04$–0.06 m s^{-1}. At high aeration rates, Bo remains almost constant with respect to the aeration rate. An increase in the A_D/A_R ratio diminishes the axial dispersion in the reactor and this results in higher Bodenstein numbers. In addition, EALR-P exhibits higher values of Bo than EALR-L. These variations of the dispersion num-

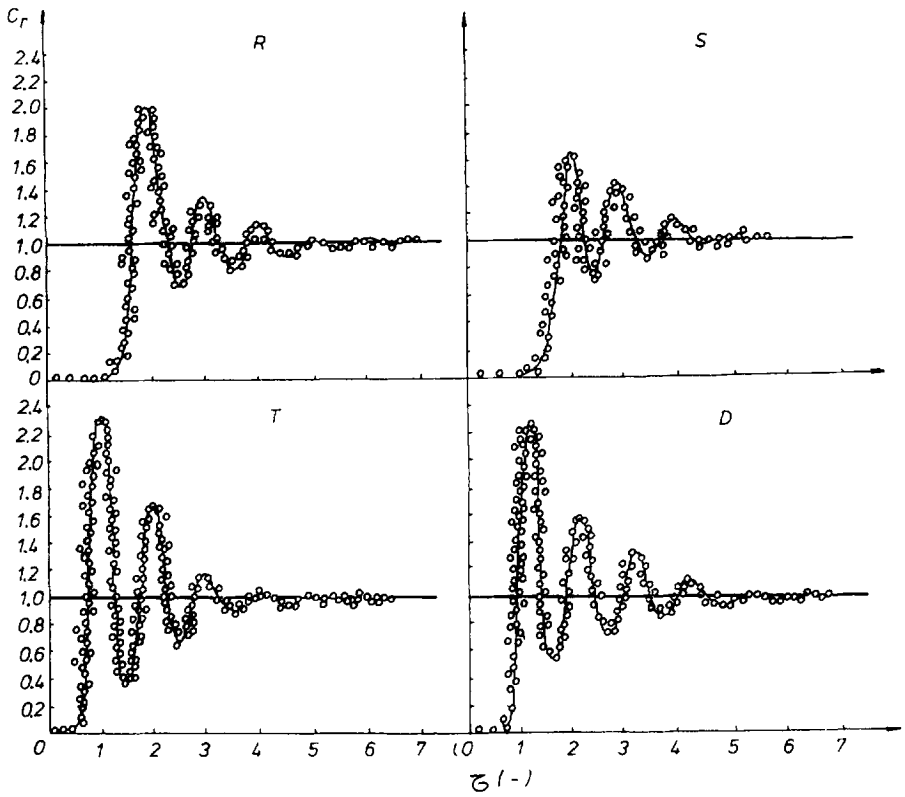

Fig. 9. The response curves to an initial Dirac signal for the reactor as a whole and the separate sections.

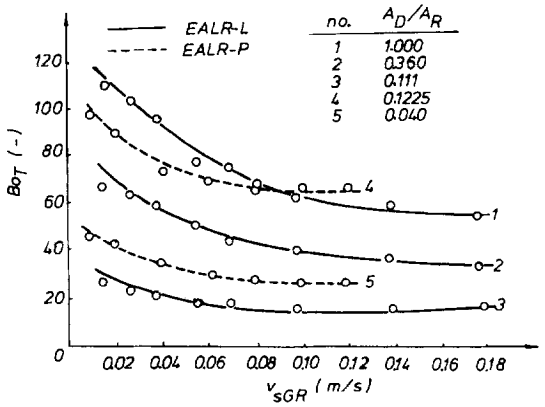

Fig. 10. Bodenstein number vs. gas superficial velocity in the overall external-loop airlift reactors.

ber Bo with the operating parameters can be attributed to the effect of the recirculating liquid velocity, which should be considered as a measure of the effective energy in the reactor. This hydrodynamic parameter is incorporated in the mean Reynolds number, Re_T. There is a significant dependence of Bo for the overall EALRs on Re_T, as shown in Fig. 11. Bo greatly decreases with increasing Re_T. The A_D/A_R ratio is the parameter which most strongly affects Bo, owing to the effect exerted by it on the liquid circulation velocity.

Fig. 12 illustrates the effect of the Reynolds number on the axial dispersion coefficient of the EALR as a whole. It is evident that D_{ax} increases with increasing Reynolds number and decreases with increasing A_D/A_R ratio.

Each of the three different sections of the airlift reactors exhibits different mixing behaviour. The downcomer shows the highest Bo numbers mainly due to the single-phase flow in this part. The riser has a somewhat better mixing performance as a result of the presence of the gas phase which induces flow patterns on a small scale in the space between the riser wall and the large bubbles (Taylor bubbles in slug two-phase flow in EALR-L, cap bubbles in churn–turbulent flow in EALR-P), followed by local mixing in bubble wakes. Mixing is significant in the top section, where bubble disengagement and reversion of the flow direction from the riser to the downcomer create considerable turbulence, resulting in low Bod-

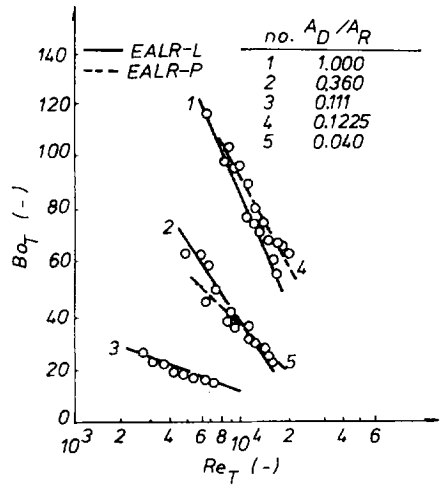

Fig. 11. Dependence of Bo on Re_T for the overall external-loop reactors.

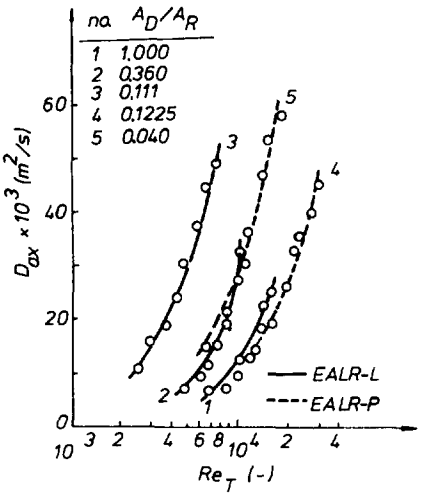

Fig. 12. Axial dispersion coefficient D_{ax} for the overall reactor vs. the Reynolds number Re_T.

enstein numbers. The top section is an extension of the riser, and so its mixing behaviour sometimes approaches that of the riser, especially at lower A_D/A_R ratios.

When the gas superficial velocity increases, the Bo numbers for the separate zones of the airlift reactors decrease, especially up to 0.04–0.06 m s^{-1} (Fig. 13), while the corresponding axial dispersion coefficient increases (Fig. 14). For the reactor as a whole, this is the result of a parallel increase in the liquid circulation velocity. In the downcomer, an increase in the A_D/A_R value causes a decrease in the liquid velocity, which contributes to a reduction in the number of large eddies which are the prime cause of axial dispersion. This explains why, for $A_D/A_R = 1$, the downcomer exhibits the greatest value of Bo (Fig. 13), while the Bo value in the riser is roughly 20% less than in the downcomer, mainly due to the two-phase flow in the riser. In addition, an increase in the A_D/A_R ratio causes an increase in the liquid velocity and a reduction in the gas holdup in the riser, which diminishes the axial dispersion. As a result, Bo is significantly higher for $A_D/A_R = 1$ compared with $A_D/A_R = 0.111$ (Fig. 13).

In the top section, where EALR-L and EALR-P are almost completely deaerated, the gas holdup causes a rise in the liquid level, which reduces the local liquid velocity. Therefore turbulence induced by liquid flow will decrease, while turbulence induced by gas disengagement will be enhanced. Apparently, these effects counterbalance the dispersion in the top section, so that the axial dispersion in this section remains almost constant for normal gas flow rates. Similar results were obtained by Verlaan [1].

The response curves to Dirac signals analysed in accordance with the axial dispersion model suggest a relation between the mixing times and Bodenstein numbers. In Fig. 2, the maxima and minima of the impulse distribution are connected by envelope curves, which are approximately exponential functions. The following empirical equation gives a good approximation to the experimental results, using the relative mixing time τ_r

$$\tau_r = \mathrm{Bo}\frac{1.931 - \ln i}{68.97} \tag{5}$$

Eq. (5) was found by regression analysis for parameters having the experimental ranges given following Eq. (4); $i = 0.05$–0.20 and Bo = 6–100, with a correlation coefficient $r = 0.832$.

The experimental results on the dispersion number reported in this work are in agreement with those presented by other researchers, as shown in Table 2.

4. Conclusions

Mixing in external-loop airlift reactors is essentially correlated with the liquid circulation velocity. The presence of air increases the mixing rate, although mixing decreases with

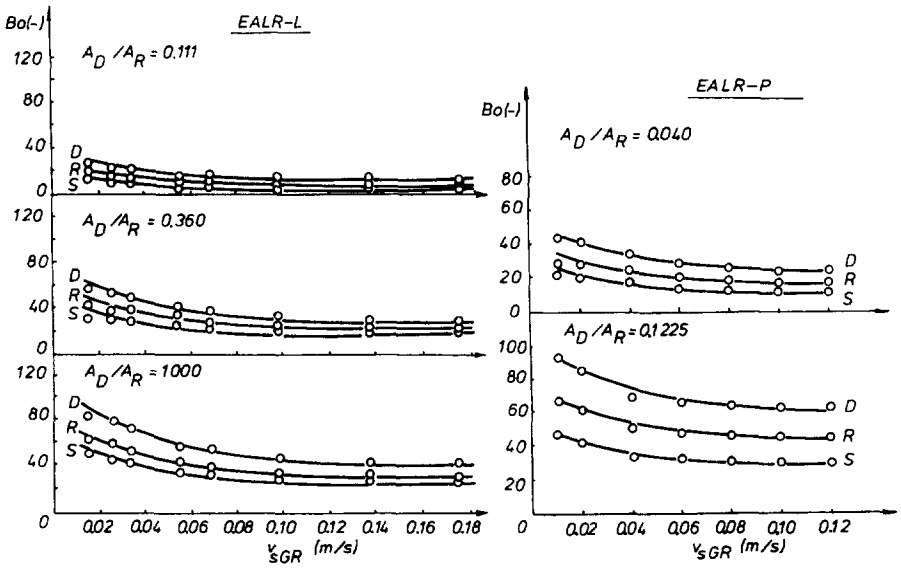

Fig. 13. Bodenstein number vs. the gas superficial velocity in the separate zones of EALRs.

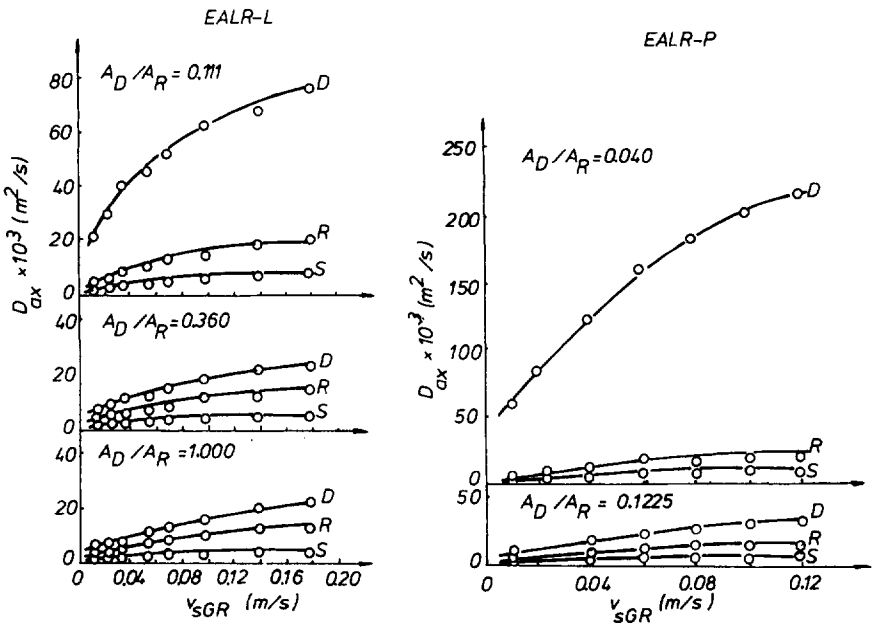

Fig. 14. Axial dispersion coefficient D_{ax} in the separate zones of EALRs.

Table 2
Values of the Bodenstein number reported in the literature

Reactor type	Gas velocity range v_{sGR} (m s^{-1})	Bo range	Reference
Concentric draft-tube internal-loop	0.05–0.30	30–60 (draft-tube region)	[19]
External-loop	0.005–0.05	30–60 (upflow region)	[18]
External-loop with supplementary gas sparger in downcomer	0.005–0.03	70–80	[7]
External-loop	0.01–0.14	40–60 (overall reactor) 30–40 (riser) 40–50 (downcomer) 10 (top section)	[1]
Internal-loop (three-phase)	0.001–0.01	5–50 (riser) 20–60 (downcomer) 0.17–5 (top section)	[20]
Internal-loop	0.01–0.15	50–80 (overall reactor) 20–30 (riser) 40–60 (downcomer) 10 (top section) 10–20 (bottom section)	[10]
External-loop	0.01–0.18	8–67 (riser) 14–93 (downcomer) 6–48 (top section)	This work

increasing liquid circulation velocity. The mixing time and axial dispersion number represent two significant ways to investigate mixing in EALRs.

A value of 95% of the complete mixing time corresponds to a maximum of about eight circulations; however, the axial dispersion is sufficiently small that the liquid flow in the riser and downcomer sections can be analysed as plug flow with axial dispersion, while the top section approaches ideal mixing. The number of circulations required to achieve this degree of mixing diminishes when the liquid circulation is impeded and appears to be proportional to the Bodenstein number.

The decrease in the Bodenstein number with decreasing A_D/A_R ratio is a consequence of the transition of airlift to bubble column flow in the riser section. This is the result of decreased convective transport as the liquid circulation is impeded. A simple correlation between the specific mixing time t_M/V_L and the principal operating and geometrical parameters has been developed, which may be useful for scale-up and design purposes, when the best compromise conditions must be determined taking into account the mixing requirements of the chemical or biological process to be achieved in the reactor.

Appendix A. Nomenclature

A_D downcomer cross-sectional area (m^2)
A_R riser cross-sectional area (m^2)

Bo	$(=(v_L L)/D_{ax})$, Bodenstein number
$C(t)$	actual concentration of tracer (kg m^{-3})
C_r	$(=C(t)/C)$, relative (dimensionless) concentration of tracer
C_∞	equilibrium concentration, resulting after complete mixing (kg m^{-3})
D_{ax}	axial dispersion coefficient (m^2 s^{-1})
D_c	$(=(D_R^2+D_D^2)^{0.5})$, mean reactor diameter (m)
D_D	downcomer diameter (m)
D_R	riser diameter (m)
H_D	ungassed liquid height in downcomer (m)
H_d	dispersion height (m)
H_R	ungassed liquid height in riser (m)
i	inhomogeneity (%)
L	length of the region under axial dispersion investigation (m)
Re_T	$(=(v_L D_c)/\nu)$, mean Reynolds number
t	current time (s)
t_C	circulation time (s)
t_M	mixing time (s)
V_R	liquid volume in the riser (m^3)
V_L	liquid volume in the reactor (m^3)
v_L	linear liquid velocity (m s^{-1})
v_{sGR}	gas superficial velocity (m s^{-1})
v_{sLR}	liquid superficial velocity (m s^{-1})
x	$(=z/L)$, dimensionless axial coordinate
z	axial coordinate (m)
ν	kinematic viscosity (m^2 s^{-1})
τ	$(=t/t_C)$, dimensionless time
τ_r	$(=t_M/t_C)$, relative mixing time
D	downcomer
R	riser
S	gas separator
T	overall reactor

References

[1] P. Verlaan, Modelling and characterization of an airlift loop bioreactor, *Ph.D. Thesis*, Wageningen University, 1987.

[2] M.H. Siegel, M. Hallaile and J. Merchuk, Air-lift reactors: design, operation and applications, in *Upstream Processes, Equipment and Techniques*, Alan R. Liss, New York, 1988, p. 79.

[3] C.H. Lin, B.S. Fang, C.S. Wu, T.F. Kuo and C.Y. Hu, Oxygen transfer and mixing in a tower cycling fermentor, *Biotechnol. Bioeng., 18* (1976) 1557.

[4] U. Onken and P. Weiland, Hydrodynamic and mass transfer in an airlift loop fermenter, *Eur. J. Appl. Microbiol. Biotechnol., 10* (1980) 31.

[5] R. Bello, C.W. Robinson and M. Moo-Young, Liquid circulation and mixing characteristics of airlift contactors, *Can. J. Chem. Eng., 62* (1984) 573.

[6] M. Popovic and C.W. Robinson, Mixing characteristics of external-loop airlifts: non-Newtonian systems, *Chem. Eng. Sci., 48* (1993) 1405.

[7] R.G.J.M. van der Lans, Hydrodynamics of a bubble column loop reactor, *Ph.D. Thesis*, Technical University of Delft, 1985.

[8] P.R. Fields and N.K.H. Slater, Tracer dispersion in a laboratory airlift reactor, *Chem. Eng. Sci., 38* (1983) 647.

[9] H.J. Warnecke, J. Pruss and H. Langemann, On a mathematical model for loop reactors, I. Residence time distribution, moments and eigenvalues, *Chem. Eng. Sci., 40* (1985) 2321.

[10] W.-J. Lu, S.-J. Hwang and C.-M. Chang, Liquid mixing in two- and three-phase airlift reactors, *Chem. Eng. Sci., 49* (1994) 1465.

[11] J.C. Merchuk and R. Yunger, The role of the gas–liquid separator of airlift reactors in mixing processes, *Chem. Eng. Sci., 45* (1990) 2973.

[12] M.Y. Chisti, *Airlift Bioreactors*, Elsevier, London, 1989.

[13] O. Levenspiel, *Chemical Reaction Engineering*, Wiley, New York, 1972.

[14] M. Gavrilescu and R.Z. Tudose, Study of liquid circulation velocity in external-loop airlift bioreactors, *Bioprocess Eng., 14* (1995) 33.

[15] M. Gavrilescu and R.Z. Tudose, Effects of downcomer-to-riser cross sectional area ratio on operation behaviour of external-loop airlift bioreactors, *Bioprocess Eng., 15* (1996) 77.

[16] J. Rousseau and J.D. Bu'Lock, Mixing characteristics of a simple airlift, *Biotechnol. Lett., 2* (1980) 475.

[17] M. Gavrilescu and R.Z. Tudose, Effects of geometry on hydrodynamics in external-loop airlift reactors, *Chem. Eng. Commun., 156* (1996) 89.

[18] P. Weiland, Untersuchung eines Airliftreaktors mit äusserem Umlauf im Hinblick auf seine Anwendung als Bioreactor, *Thesis*, University of Dortmund, 1978.

[19] R.T. Hatch, Experimental and theoretical studies of oxygen transfer in the airlift fermentor, *Thesis*, MIT Cambridge, MA, 1973.

[20] B. Obradovic, A. Dudukovic and G.V. Novakovic, Local and overall mixing characteristics of the gas–liquid–solid airlift reactor, *Ind. Eng. Chem. Res., 33* (1994) 698.